Geochemical Perspectives Letters EAG

Nitrogen isotopic variations in the early Solar System recorded by pallasites

J. Gamblin[1*], E. Füri[1], B. Luais[1], L. Zimmermann[1]

https://doi.org/10.7185/geochemlet.2607

Abstract

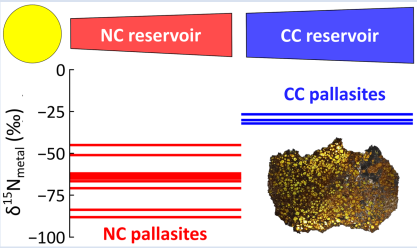

To gain new insights into nitrogen (N) isotopic variations in the early Solar System, N and noble gas (Ne, Ar) isotopes were measured in metal fragments and olivine separates from thirteen pallasites and five IIIAB iron meteorites. While $\delta^{15}N$ values in olivine are affected by cosmogenic ^{15}N, as demonstrated by cosmogenic ^{21}Ne abundances, the $\delta^{15}N$ values of metal phases reflect reservoir signatures rather than secondary processes. Non-carbonaceous (NC) pallasites have lower $\delta^{15}N$ values (−88.86 ± 0.90 ‰ to −45.04 ± 0.91 ‰) than carbonaceous (CC) pallasites (−34.03 ± 0.69 ‰ to −26.12 ± 0.64 ‰), indicating their parent bodies accreted isotopically distinct N-bearing precursors in the inner and outer regions of the protoplanetary disk. The $\delta^{15}N$ variations within each reservoir also suggest N isotopic heterogeneity at a smaller scale. While NC irons and NC pallasites exhibit overlapping $\delta^{15}N$ values, CC pallasites are less ^{15}N-rich than CC irons, implying that their parent bodies accreted in different locations and/or at different times within the outer disk.

Received 26 September 2025 | Accepted 19 December 2025 | Published 17 February 2026

Introduction

Non-carbonaceous (NC) and carbonaceous (CC) chondrites, whose parent bodies accreted in the inner and outer Solar System, respectively, are distinguished by characteristic nucleosynthetic isotope anomalies (*e.g.*, $\varepsilon^{54}Cr$ and $\varepsilon^{50}Ti$; Trinquier *et al.*, 2009; Warren, 2011). However, their $\delta^{15}N$ values (defined as the per mille deviation from the modern atmospheric $^{15}N/^{14}N$ ratio of 3.6765×10^{-3}; Nier, 1950) largely overlap (−57.3 ‰ to +39.3 ‰ for NC chondrites, excluding two outliers, and −45.0 ‰ to +76.2 ‰ for CC chondrites, excluding the ^{15}N-rich CR chondrites and other atypical ^{15}N-rich chondrites such as CB, CH, or Bells; based on a compilation of previous work available at Füri and Lastes (2025). In contrast, magmatic iron meteorites show clearer differences in N isotopic compositions between those linked to inner and outer Solar System parent bodies. NC-type irons predominantly record negative $\delta^{15}N$ values (although they show an overall range from −95.8 ‰ to +46.7 ‰), while CC irons record mostly positive $\delta^{15}N$ values (−16.3 ‰ to +155.6 ‰; based on a compilation of previous work available at Füri and Gamblin (2025); Table S-5).

Magmatic iron meteorites originate from the cores of the earliest formed planetesimals, which accreted within the first Myr after calcium-aluminium-rich inclusion (CAI) formation (Spitzer *et al.*, 2021). Since N isotopes are not significantly fractionated between metal and silicate during planetary differentiation (only a few per mille; Grewal *et al.*, 2022) and between solid and liquid metal during core crystallisation (≲1.2 ‰; Grewal *et al.*, 2025), the N isotopic compositions of most magmatic irons reflect those of their parent bodies at the time of differentiation. By that stage, thermal metamorphism could already have altered the initial N isotopic compositions. However, since both NC and CC irons record the end stage of thermal evolution, their different $\delta^{15}N$ values suggest that their parent bodies — the earliest planetesimals in the inner and outer protoplanetary disk — accreted N carriers with distinct isotopic compositions (Grewal *et al.*, 2021, 2025). The metal phase of meteorites is particularly well suited for tracking these N isotopic signatures, as N is siderophile under the redox conditions estimated for the differentiation of the parent bodies of iron meteorites (Grewal *et al.*, 2021, 2024) and pallasites (Righter *et al.*, 1990, 2016). Since pallasites may be genetically linked with irons (particularly the main group pallasites, hereon PMG, with IIIAB irons), they can provide additional insights into N isotopic variations within the protoplanetary disk during the earliest stages of Solar System history.

Pallasites are stony iron meteorites mainly composed of Fe-Ni metal and silicates (olivine ± pyroxene). While generally considered mixtures of core- and mantle-derived material, their formation process remains debated. Proposed models suggest formation at the core-mantle interface or at shallower depths within a differentiated planetesimal (*e.g.*, Boesenberg *et al.*, 2012; Teplyakova *et al.*, 2022), or through impact mixing of core metal with mantle olivines from two distinct planetesimals (*e.g.*, Yang *et al.*, 2010; Windmill *et al.*, 2022). These processes may have occurred multiple times in different regions of the Solar System, as indicated by variations in O isotopic compositions that point to distinct pallasite parent bodies (Fig. S-1; Boesenberg *et al.*, 2012). Some pallasites are linked to the inner Solar System and the NC reservoir, while others are associated with the outer Solar System and the CC reservoir (Warren, 2011; Boesenberg *et al.*, 2016; Hilton *et al.*, 2019; Kruijer *et al.*, 2022). Like iron meteorites, their metal phases are interpreted to trace

1. Université de Lorraine, CNRS, CRPG, F-54000 Nancy, France
* Corresponding author (email: julie.gamblin@univ-lorraine.fr)

N isotopic variations between these reservoirs. However, $\delta^{15}N$ measurements of pallasites remain scarce (Prombo and Clayton, 1993; Mathew *et al.*, 2000) and do not encompass all pallasite groups or types. In particular, $\delta^{15}N$ data for the metal phase of CC pallasites and pyroxene-rich pallasites are currently lacking. This study aims to provide a comprehensive overview of the N isotopic composition of NC and CC pallasites to better constrain the N isotopic distribution and evolution in the early protoplanetary disk.

Material and Methods

Thirteen pallasites were analysed for this study (see details in Supplementary Information). These include eight PMG (NC reservoir): six typical PMG (Admire, Brahin, Esquel, Fukang, Imilac, and Seymchan) and two with anomalous metal compositions (PMG–am, for anomalous metal; Brenham and Pavlodar). The sample suite also comprises two Eagle Station pallasites (PES; Eagle Station and Karavannoe; CC reservoir), two pyroxene pallasites (Px pall.; Vermillion and NWA 10019; NC reservoir), and one ungrouped pallasite associated with the CC reservoir (Milton). These pallasites likely originate from four or five different parent bodies — two or three from the NC reservoir and two from the CC reservoir. Five IIIAB magmatic iron meteorites (Bear Creek, Cape York, Grant, Owens Valley, and Trenton) were also analysed to investigate their possible genetic link to PMG. To ensure accurate analysis, pure metal fragments were carefully selected, with surface oxidation removed *via* acid treatment, while olivine grains free of other phases, inclusions, and alteration were also isolated. Descriptions of each analysed pallasite and IIIAB iron meteorite, along with details of the sample preparation, are provided in the SI.

Nitrogen was extracted from metal fragments and pure olivine separates by stepped CO_2 laser-heating, and its abundances and isotope ratios were analysed with a Noblesse-HR noble gas mass spectrometer at the noble gas facility of the Centre de Recherches Pétrographiques et Géochimiques (CRPG). Notably, $^{15}N_{cosm}$ is produced from ^{16}O by cosmic ray-induced spallation during space exposure (*e.g.*, Mathew and Murty, 1993). Since oxygen is virtually absent in the metal phase of pallasites and in magmatic iron meteorites, the cosmogenic contribution to the measured $\delta^{15}N$ in metals is negligible. However, this contribution can significantly modify the $\delta^{15}N$ values of silicates. To address this, noble gas (Ne and Ar) abundances and isotope ratios were analysed alongside N to quantify any cosmogenic nuclide contributions, estimate the cosmic ray exposure (CRE) ages of the meteorites based on Ne isotopes, and correct the $\delta^{15}N$ of olivines for cosmogenic ^{15}N contributions. Detailed descriptions of the analytical procedure, data treatment, and correction for cosmogenic ^{15}N are provided in the SI. A limitation of the applied method is that the metal fragments could not be melted by the laser heating, potentially influencing the efficiency of N and noble gas extraction. Consequently, concentrations for the metal phases may not have been quantitatively constrained. Thus, the following discussion primarily focuses on the isotope ratios of N (-Ne-Ar).

Results

Neon extracted from metal fragments and olivine separates of pallasites in this study, as well as in previous studies (*e.g.*, Schultz and Franke, 2004), is predominantly cosmogenic, as indicated by $^{20}Ne/^{22}Ne$ and $^{21}Ne/^{22}Ne$ ratios close to unity (Fig. S-5). No solar Ne contributions were detected. The extracted Ar is also predominantly cosmogenic, with $^{36}Ar/^{38}Ar$ ratios mostly ranging between 0.63 and 0.72. The amount of ^{21}Ne released from the olivine separates suggests CRE ages ranging from 3 Myr to ∼174 Myr (Table S-3). Spallation reactions induced by galactic cosmic rays have thus significantly modified the N isotopic compositions of the silicate phases (Table S-4), in clear contrast to the metal phases, whose $\delta^{15}N$ remained unaffected by cosmogenic ^{15}N (see details in the SI). Consequently, the $\delta^{15}N$ values of olivines will not be discussed further, and this study focuses on the N isotopic compositions of metal.

Figure 1 displays the $\delta^{15}N$ values measured in the metal phases of pallasites and IIIAB iron meteorites. While Figure S-4 shows the results of all individual extraction steps, Figure 1 presents the abundance-weighted averages, providing a single $\delta^{15}N$ value for each analysed fragment. Symbol sizes scale with the N abundances extracted *per* mass and are comparable to concentrations reported in the literature, indicating efficient N extraction from the samples. No correlation is observed between N yield and $\delta^{15}N$ values. The N abundances extracted *per* mass from CC pallasite samples fall within the range measured for NC pallasites. A wide range of $\delta^{15}N$ values is observed in pallasites, with distinct values for the different pallasite groups, all significantly higher than the solar nebula value (−383 ± 8 ‰; Marty *et al.*, 2011). The measured values are consistent with literature data, demonstrating that any incomplete N extraction did not result in significant isotopic fractionation. The $\delta^{15}N$ values of PMG range from −88.86 ± 0.90 ‰ for Brenham to −17.38 ± 1.44 ‰ for Fukang. However, the highest value measured in Fukang may be considered an outlier. Only a small amount of N was extracted from this fragment, and analysis of a second metal fragment yielded a value more consistent with the other PMG (−70.86 ± 1.02 ‰), suggesting that the elevated value resulted from significant blank contribution that was not fully corrected. The PMG-am Brenham shows significant isotopic variations among the three fragments analysed (−47.94 ± 0.96 ‰, −56.57 ± 1.19 ‰, and −88.86 ± 0.90 ‰). Since this sample was particularly weathered, the elevated $\delta^{15}N$ values may result from incomplete removal of surface weathering (Fig. S-2). Excluding the Fukang outlier, the $\delta^{15}N$ values of the "normal" PMG fall within a narrower range, from −70.86 ± 1.02 ‰ to −48.94 ± 0.89 ‰,

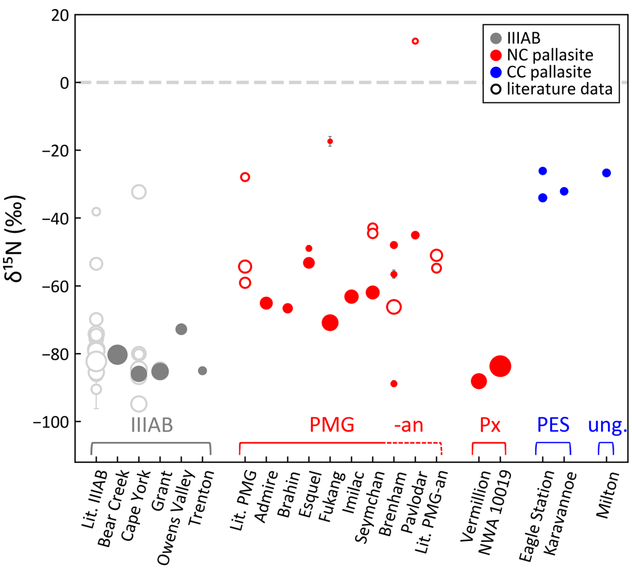

Figure 1 $\delta^{15}N$ of metal from pallasites and IIIAB iron meteorites. Symbol sizes are correlated to the N abundances extracted per mass. Uncertainties are 1σ, and error bars are, in most cases, smaller than symbol sizes. Literature data sources are listed in Table S-5.

consistent with most literature values. Interestingly, PMG generally exhibit higher $\delta^{15}N$ values than IIIAB (–85.97 ± 0.59 ‰ to –72.81 ± 0.62‰), which are also in agreement with previous data (see references in Table S-5). The $\delta^{15}N$ variations within the PMG group and the IIIAB group may reflect N isotopic heterogeneities among the small fragments analysed, possibly caused by minor inclusions within the metal.

Pyroxene pallasites are depleted in ^{15}N compared to "normal" PMG, with $\delta^{15}N$ values of –88.11 ± 1.02 ‰ for Vermillion and –83.67 ± 0.92 ‰ for NWA 10019. Surprisingly, they have similar N isotopic compositions, whereas their different O isotopic compositions indicate an origin from distinct parent bodies (Fig. S-1; Boesenberg *et al.*, 2016). These values fall within the range of IIIAB meteorites analysed in this study. In contrast, the PES group is enriched in ^{15}N compared to both PMG and pyroxene pallasites, with $\delta^{15}N$ values ranging from –34.03 ± 0.69 ‰ to –26.12 ± 0.64 ‰. Milton's $\delta^{15}N$ value also falls within this range (–26.67 ± 0.71 ‰). Overall, the new results reveal that CC pallasites (–34.03 ± 0.69 ‰ to –26.12 ± 0.64 ‰) have higher $\delta^{15}N$ values compared to NC pallasites (–88.86 ± 0.90 ‰ to –45.04 ± 0.91 ‰).

Discussion

Like iron meteorites, pallasite metals are thought to preserve the N isotopic composition of their bulk parent bodies at the time of differentiation. This inference is based on experimental evidence showing that neither core-mantle differentiation (Grewal *et al.*, 2022) nor fractional crystallisation of liquid metal (Grewal *et al.*, 2025) significantly alters N isotope ratios, as outlined in the Introduction. Prior to melting and differentiation, thermal metamorphism can preferentially remove ^{15}N-rich components from planetesimals (Grewal *et al.*, 2025). However, as for iron meteorites, the metals of both NC and CC pallasites represent the end stage products of thermal evolution. Because their parent bodies experienced similarly high temperatures at which N carrier phases were largely decomposed and melted, the observed $\delta^{15}N$ differences between NC and CC pallasites cannot be attributed to selective destruction or preservation of different N carriers during thermal metamorphism. Aqueous alteration may also have occurred in pallasite parent bodies prior to differentiation. The marginally higher oxidation state of PES (IW +0.5; Righter *et al.*, 1990) compared to PMG (IW −1 to −0.5; Righter *et al.*, 2016) may indicate greater water-ice accretion on the PES parent body, increasing the potential for such processing. However, aqueous alteration of undifferentiated material typically leads to preferential removal of ^{15}N (Broadley *et al.*, 2023), which contrasts with observations in pallasites, where the most oxidised parent body shows a higher $\delta^{15}N$.

Another possibility is that the pallasite formation process itself affected the $\delta^{15}N$ values. This process remains debated, with some models suggesting it involved impact related disruption of a differentiated body (*e.g.*, Yang *et al.*, 2010). If N isotope fractionation had occurred through evaporation or degassing of molten metal during impact events, it should have been accompanied by a loss of volatile siderophile elements such as Ge and Ga, together with preferential loss of the lighter ^{14}N isotope. Such a process would therefore be expected to produce a negative correlation between $\delta^{15}N$ values and Ge and Ga concentrations in metal samples originating from the same parent body — particularly within the PMG and IIIAB groups, or when comparing PMG to IIIAB. However, no such correlation is observed (Fig. S-7), indicating that degassing did not significantly affect $\delta^{15}N$ values. Consequently, thermal metamorphism, aqueous alteration, and impact processes are unlikely to account for the $\delta^{15}N$ differences observed between NC and CC pallasites, strongly supporting the interpretation that these variations reflect distinct primary reservoir signatures rather than secondary effects. Pallasite parent bodies in the NC and CC reservoirs are therefore inferred to have accreted isotopically distinct N-bearing phases, supporting the idea — first proposed based on iron meteorites (Grewal *et al.*, 2021, 2025) — that isotopic heterogeneity in N existed between the inner and outer regions of the protoplanetary disk.

Figure 2 shows O isotopic anomalies in pallasite silicates and Mo nucleosynthetic anomalies in both pallasite metal and magmatic iron meteorite groups as a function of their N isotopic compositions measured in metal. These anomalies, along with others (*e.g.*, Cr, Ti, Ru), have been key in distinguishing between the NC and CC reservoirs (*e.g.*, Warren, 2011; Kruijer *et al.*, 2017, 2022). Molybdenum, a moderately siderophile and refractory element, is particularly useful because it is readily measurable in metal and exhibits a well resolved isotopic dichotomy between the two reservoirs (Spitzer *et al.*, 2020). In Figure 2b, pallasites and irons from the NC and CC reservoirs are clearly separated by their $\Delta^{95}Mo$ values, while their $\delta^{15}N$ values show partial overlap, with NC samples extending to more ^{15}N depleted values and CC samples to higher $\delta^{15}N$ values. A wide range of $\delta^{15}N$ values is observed among the different parent bodies within each reservoir. Whereas the ^{14}N depletion of the NC iron group IVA could reflect impact induced fractionation (Grewal *et al.*, 2025), the overall variations likely result from isotopic heterogeneity in the N carrier phase(s) within each reservoir. These variations could arise from i) temporal or spatial evolution in the $\delta^{15}N$ of a single phase (*e.g.*, organic matter), and/or ii) the coexistence of multiple isotopically distinct N carriers (including organics, nitrides, ammonia ice), whose relative abundances were controlled by disk physicochemical conditions and were accreted in varying proportions by planetesimals. Notably, CC pallasites do not align with CC iron meteorites (Fig. 2b). The two parent bodies of the CC pallasites show very similar $\delta^{15}N$ values, as do the four parent bodies of the CC iron meteorites (excluding the particularly ^{15}N-rich IIC parent body), but CC pallasites display negative $\delta^{15}N$ values — distinct from the predominantly positive values of CC iron meteorites — while retaining similar Mo nucleosynthetic anomalies. This implies that CC pallasites and CC irons originated from distinct parent bodies that may have accreted in separate locations and/or at different times in the outer Solar System. The more oxidising conditions recorded by PES (IW +0.5; Righter *et al.*, 1990) compared to CC irons (IW −2 to IW −1; Grewal *et al.*, 2024) could indicate that the PES parent body accreted more water ice, possibly farther from the Sun, supporting this hypothesis. Determining the relative accretion times and locations of the parent bodies of CC pallasites and CC iron meteorites will be key to confirming this. Currently, the parent body of the Eagle Station pallasite is believed to have differentiated within the first 4 Myr after CAI formation (Luu *et al.*, 2014), though its precise accretion time remains poorly constrained and may have spanned several million years. In comparison, the parent bodies of CC iron meteorites are thought to have differentiated between 3 and 4 Myr after CAI formation (Spitzer *et al.*, 2021), and may have accreted either as early as the parent bodies of NC iron meteorites (within the first Myr after CAI formation; Spitzer *et al.*, 2021) or slightly later (Grewal *et al.*, 2024). In contrast, NC pallasites and NC iron meteorites exhibit consistent Mo nucleosynthetic anomalies as well as overlapping N isotopic compositions. Their $\delta^{15}N$ variations may also reflect isotopic heterogeneity in the N-bearing phases within the NC reservoir. However, unlike the parent bodies from the CC reservoir, there is no evidence that the parent bodies of NC pallasites and NC iron meteorites accreted distinctly different N carrier

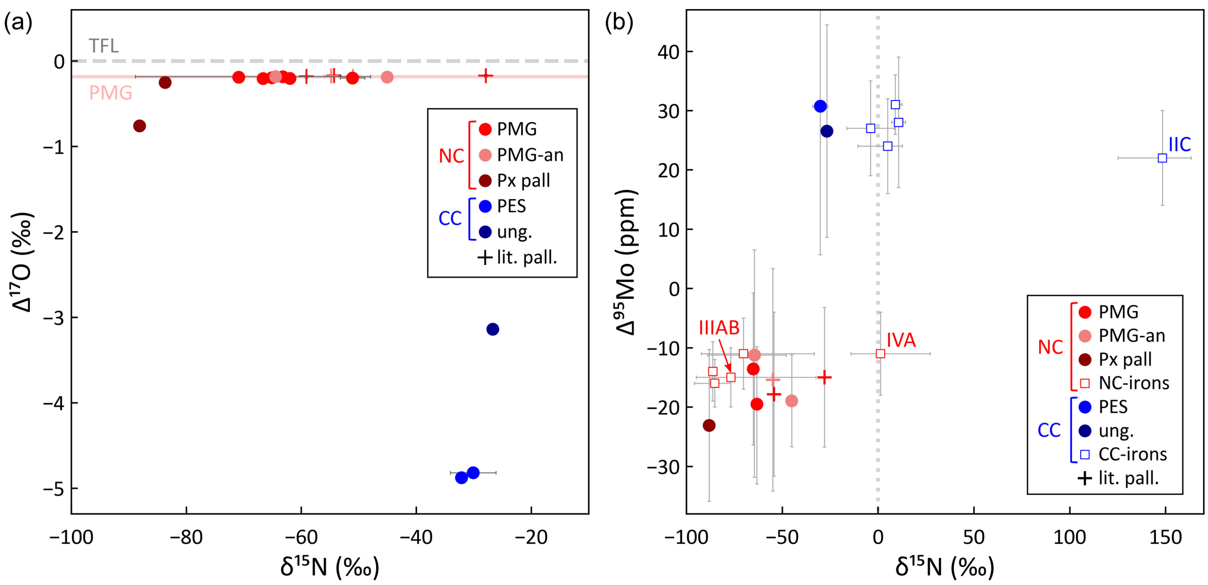

Figure 2 **(a)** Oxygen isotopic anomalies ($\Delta^{17}O = \delta^{17}O - 0.52 \times \delta^{18}O$, *i.e.* the deviation from the terrestrial fractionation line in a $\delta^{17}O$ *versus* $\delta^{18}O$ diagram) and **(b)** Mo nucleosynthetic anomalies ($\Delta^{95}Mo = (\varepsilon^{95}Mo - 0.596 \times \varepsilon^{94}Mo) \times 100$; Spitzer *et al.*, 2020) of pallasites and iron meteorites *versus* their N isotopic compositions. Iron meteorite data points represent average values for each group originating from specific parent bodies, while pallasite data points correspond to average values of individual meteorites. Meteorites and groups from the NC and CC reservoirs are shown in different shades of red and blue, respectively. The dashed line in (a) marks the terrestrial fractionation line (TFL), and the dotted line in (b) indicates $\delta^{15}N = 0$ ‰. Error bars for $\delta^{15}N$ represent the range of values for both pallasites and iron meteorites. For pallasites, error bars for $\Delta^{17}O$ and $\Delta^{95}Mo$ similarly represent the range of literature data, including the large 1σ uncertainties for $\Delta^{95}Mo$. For iron meteorites, $\Delta^{95}Mo$ values are taken from Spitzer *et al.* (2020), with uncertainties corresponding to the 95 % confidence intervals. Literature data sources are listed in Table S-5.

phases, or that they formed in clearly separate locations and/or at different times.

Acknowledgements

This work was funded by the European Union (ERC, IRONIS, 101087562, awarded to EF). Views and opinions expressed are however those of the author(s) only and do not necessarily reflect those of the European Union or the European Research Council. Neither the European Union nor the granting authority can be held responsible for them. We thank the various museums and meteorite sellers cited in Table S-1 for providing the samples for this study, as well as Bouchaïb Tibari and Allan Bauer for their assistance with the noble gas analyses at CRPG. We are also grateful for the constructive reviews provided by Seann McKibbin and Conel Alexander, and to Francis McCubbin for editorial handling. This is CRPG contribution 2881.

Editor: Francis McCubbin

Additional Information

Supplementary Information accompanies this letter at https://www.geochemicalperspectivesletters.org/article2607.

Cite this letter as: Gamblin, J., Füri, E., Luais, B., Zimmermann, L. (2026) Nitrogen isotopic variations in the early Solar System recorded by pallasites. *Geochem. Persp. Let.* 39, 17–21. https://doi.org/10.7185/geochemlet.2607

References

Boesenberg, J.S., Delaney, J.S., Hewins, R.H. (2012) A petrological and chemical re-examination of Main Group pallasite formation. *Geochimica et Cosmochimica Acta* 89, 134–158. https://doi.org/10.1016/j.gca.2012.04.037

Boesenberg, J.S., Mayne, R.G., Humayun, M., Silver, A.P., Greenwood, R.C., Franchi, I.A. (2016) Pyroxene-Plagioclase Pallasite Northwest Africa 10019: Where Does It Belong? *47th Lunar and Planetary Science Conference*, 2297.

Broadley, M.W. *et al.* (2023) The noble gas and nitrogen relationship between Ryugu and carbonaceous chondrites. *Geochimica et Cosmochimica Acta* 345, 62–74. https://doi.org/10.1016/j.gca.2023.01.020

Buseck, P.R., Goldstein, J.I. (1969) Olivine Compositions and Cooling Rates of Pallasitic Meteorites. *Geological Society of America Bulletin* 80, 2141. https://doi.org/10.1130/0016-7606(1969)80[2141:OCACRO]2.0.CO;2

Füri, E., Gamblin, J. (2025) Compilation of nitrogen isotope ratios and abundances in iron meteorites determined by step-heating or secondary ion mass spectrometry (SIMS). *OTELo Research Data Repository, ORDaR*. https://doi.org/10.24396/ORDAR-185

Füri, E., Lastes, A. (2025) Compilation of nitrogen isotope ratios and abundances in chondrites. *OTELo Research Data Repository, ORDaR*. https://doi.org/10.24396/ORDAR-190

Greenwood, R.C., Burbine, T.H., Miller, M.F., Franchi, Ian. A. (2017) Melting and differentiation of early-formed asteroids: The perspective from high precision oxygen isotope studies. *Geochemistry* 77, 1–43. https://doi.org/10.1016/j.chemer.2016.09.005

Grewal, D.S., Dasgupta, R., Marty, B. (2021) A very early origin of isotopically distinct nitrogen in inner Solar System protoplanets. *Nature Astronomy* 5, 356–364. https://doi.org/10.1038/s41550-020-01283-y

Grewal, D.S., Dasgupta, R., Hough, T., Farnell, A. (2021) Rates of protoplanetary accretion and differentiation set nitrogen budget of rocky planets. *Nature Geoscience* 14, 369–376. https://doi.org/10.1038/s41561-021-00733-0

Grewal, D.S., Sun, T., Aithala, S., Hough, T., Dasgupta, R., Yeung, L.Y., Schauble, E.A. (2022) Limited nitrogen isotopic fractionation during core-mantle differentiation in rocky protoplanets and planets. *Geochimica et Cosmochimica Acta* 338, 347–364. https://doi.org/10.1016/j.gca.2022.10.025

Grewal, D.S., Nie, N.X., Zhang, B., Izidoro, A., Asimow, P.D. (2024) Accretion of the earliest inner Solar System planetesimals beyond the water snowline. *Nature Astronomy* 8, 290–297. https://doi.org/10.1038/s41550-023-02172-w

Grewal, D.S., Bhattacharjee, S., Mardaru, G.-D., Asimow, P.D. (2025) Tracing the origin of volatiles on Earth using nitrogen isotope ratios in iron meteorites. *Geochimica et Cosmochimica Acta* 388, 34–47. https://doi.org/10.1016/j.gca.2024.11.011

Hilton, C.D., Bermingham, K.R., Walker, R.J., McCoy, T.J. (2019) Genetics, crystallization sequence, and age of the South Byron Trio iron meteorites: New insights to carbonaceous chondrite (CC) type parent bodies. *Geochimica et Cosmochimica Acta* 251, 217–228. https://doi.org/10.1016/j.gca.2019.02.035

Kruijer, T.S., Burkhardt, C., Budde, G., Kleine, T. (2017) Age of Jupiter inferred from the distinct genetics and formation times of meteorites. *Proceedings of the National Academy of Sciences* 114, 6712–6716. https://doi.org/10.1073/pnas.1704461114

Kruijer, T.S., Burkhardt, C., Borg, L.E., Kleine, T. (2022) Tungsten and molybdenum isotopic evidence for an impact origin of pallasites. *Earth and Planetary Science Letters* 584, 117440. https://doi.org/10.1016/j.epsl.2022.117440

Luu, T.-H., Chaussidon, M., Birck, J.-L. (2014) Timing of metal–silicate differentiation in the Eagle Station pallasite parent body. *Comptes Rendus Geoscience* 346, 75–81. https://doi.org/10.1016/j.crte.2014.03.004

Mathew, K.J., Murty, S.V.S. (1993) Cosmic ray produced nitrogen in extra terrestrial matter. *Journal of Earth System Science* 102, 415–437. https://doi.org/10.1007/BF02841731

Mathew, K.J., Palma, R.L., Marti, K., Lavielle, B. (2000) Isotopic signatures and origin of nitrogen in IIE and IVA iron meteorites. *Geochimica et Cosmochimica Acta* 64, 545–557. https://doi.org/10.1016/S0016-7037(99)00316-6

Marty, B., Chaussidon, M., Wiens, R.C., Jurewicz, A.J.G., Burnett, D.S. (2011) A 15 N-Poor isotopic composition for the Solar System as shown by Genesis solar wind samples. *Science* 332, 1533–1536. https://doi.org/10.1126/science.1204656

Nier, A.O. (1950) A Redetermination of the Relative Abundances of the Isotopes of Carbon, Nitrogen, Oxygen, Argon, and Potassium. *Physical Review* 77, 789–793. https://doi.org/10.1103/PhysRev.77.789

Prombo, C.A., Clayton, R.N. (1993) Nitrogen isotopic compositions of iron meteorites. *Geochimica et Cosmochimica Acta* 57, 3749–3761. https://doi.org/10.1016/0016-7037(93)90153-N

Righter, K., Arculus, R.J., Delano, J.W., Paslick, C. (1990) Electrochemical measurements and thermodynamic calculations of redox equilibria in pallasite meteorites: Implications for the eucrite parent body. *Geochimica et Cosmochimica Acta* 54, 1803–1815. https://doi.org/10.1016/0016-7037(90)90409-E

Righter, K., Sutton, S.R., Danielson, L., Pando, K., Newville, M. (2016) Redox variations in the inner solar system with new constraints from vanadium XANES in spinels. *American Mineralogist* 101, 1928–1942. https://doi.org/10.2138/am-2016-5638

Schultz, L., Franke, L. (2004) Helium, neon, and argon in meteorites: A data collection. *Meteoritics & Planetary Science* 39, 1889–1890. https://doi.org/10.1111/j.1945-5100.2004.tb00083.x

Scott, E.R.D. (1977) Pallasites—metal composition, classification and relationships with iron meteorites. *Geochimica et Cosmochimica Acta* 41, 349–360. https://doi.org/10.1016/0016-7037(77)90262-9

Spitzer, F., Burkhardt, C., Budde, G., Kruijer, T.S., Morbidelli, A., Kleine, T. (2020) Isotopic Evolution of the Inner Solar System Inferred from Molybdenum Isotopes in Meteorites. *The Astrophysical Journal Letters* 898, L2. https://doi.org/10.3847/2041-8213/ab9e6a

Spitzer, F., Burkhardt, C., Nimmo, F., Kleine, T. (2021) Nucleosynthetic Pt isotope anomalies and the Hf-W chronology of core formation in inner and outer solar system planetesimals. *Earth and Planetary Science Letters* 576, 117211. https://doi.org/10.1016/j.epsl.2021.117211

Teplyakova, S.N., Lorenz, C.A., Ivanova, M.A., Humayun, M., Kononkova, N.N., Borisovsky, S.E., Korochantsev, A.V., Franchi, I.A., Zinovieva, N.G. (2022) Karavannoe: Mineralogy, trace element geochemistry, and origin of Eagle Station group pallasites. *Meteoritics & Planetary Science* 57, 1158–1173. https://doi.org/10.1111/maps.13814

Trinquier, A., Elliott, T., Ulfbeck, D., Coath, C., Krot, A.N., Bizzarro, M. (2009) Origin of Nucleosynthetic Isotope Heterogeneity in the Solar Protoplanetary Disk. *Science* 324, 374–376. https://doi.org/10.1126/science.1168221

Warren, P.H. (2011) Stable-isotopic anomalies and the accretionary assemblage of the Earth and Mars: A subordinate role for carbonaceous chondrites. *Earth and Planetary Science Letters* 311, 93–100. https://doi.org/10.1016/j.epsl.2011.08.047

Windmill, R.J., Franchi, I.A., Hellmann, J.L., Schneider, J.M., Spitzer, F., Kleine, T., Greenwood, R.C., Anand, M. (2022) Isotopic evidence for pallasite formation by impact mixing of olivine and metal during the first 10 million years of the Solar System. *PNAS Nexus* 1, pgac015. https://doi.org/10.1093/pnasnexus/pgac015

Yang, J., Goldstein, J.I., Scott, E.R.D. (2010) Main-group pallasites: Thermal history, relationship to IIIAB irons, and origin. *Geochimica et Cosmochimica Acta* 74, 4471–4492. https://doi.org/10.1016/j.gca.2010.04.016